PCCP

Accepted Manuscript

ROYAL SOCIETY OF CHEMISTRY

www.rsc.org/pccp

Physical chemistry: Chemical Physics

ARTICLE

Assembly of polyaniline nanotubes by interfacial polymerization for corrosion protection

C. Oueiny,[a] S. Berlioz[a] and F. X. Perrin[a]

Polyaniline (PANI) was synthesized by the oxidation of aniline with ammonium peroxydisulfate as an oxidant in an immiscible organic/aqueous biphasic system and with decylphosphonic acid (DPA) or benzylphosponic acid (BPA) in the aqueous phase. Nanofibers of aniline oligomers were produced using BPA in the aqueous phase while high quality polyaniline nanotubes were produced using DPA in the aqueous phase. PANI nanotubes have a outer diameter 160-240 nm, an inner diameter of 50-100 nm and a length of the order of several µm. The understanding of the formation of PANI nanotubes was examined by isolation of reaction intermediates and their *ex situ* characterization by atomic force microscopy. The roles of BPA and DPA on the morphology formation of the PANI nanostructures were discussed. A nanofibrillar template produced by aniline oligomers was found to guide the growth of PANI to nanotubular morphology. PANI nanotubes are thus not derived from DPA vesicles. Preliminary corrosion tests exhibit high corrosion protection efficiency of PANI nanotubes because of their high surface area and corrosion inhibitive properties of DPA dopant.

Received 00th January 20xx,
Accepted 00th January 20xx

DOI: 10.1039/x0xx00000x

www.rsc.org/

1. Introduction

Beginning with the discovery of carbon nanotubes[1], materials with nanotubular structure have attracted considerable attention because of their unique properties and promising applications in molecular electronics, optics and biomedical science. Many excellent reviews have addressed the self-assembly process by which nanostructured 1D polyaniline nanotubes are generated[2-5]. Polyaniline nanofibers and nanotubes can be made by soft[6] or hard[7] template synthesis, nanofiber seeding[8], rapidly-mixed reaction[9], interfacial polymerization[9], electrochemical polymerization[10], electrospinning[11] or mechanical stretching. [12] Among these reported approaches, interfacial polymerization (IP) is a general chemical route to obtain PANI nanofibers.[13-15] Two reasons were considered to explain the formation of nanofibers by IP (1) the reduced local dielectric constant of water at the organic/water interface that would favor the formation of phenazine nucleates at the interface[16] and (2) the suppression of the secondary growth of polyaniline by removing the nanofibers from the reactive interface.[9]

PANI nanofibers are obtained by IP using a great variety of dopants (inorganic or organic acids[9,17] and/or anionic[18] or non ionic[19] surfactants) in the aqueous phase. Other morphologies obtained by IP are seldom reported.[17,18,20] Cyclic PANI nanostructures were obtained with the aid of polyacrylic acid dissolved in the water phase[21] while nanosheets were formed by controlling the diffusion rate and the polymerization induction time of aniline.[22] There are very few instances where nanotube morphology has been observed using IP. Nanotubes were formed by tuning the concentration of ammonium persulfate (APS)[23] or DL-tartaric acid in the water phase.[24] Therefore, the synthesis of high-quality PANI nanotubes remains a challenge to material scientists. Here we report the formation of high-quality PANI nanotubes by interfacial oxidation polymerization of aniline with the aid of decylphosphonic acid (PANI-DPA). The influence of the organophosphonic acid on the morphology of PANI was investigated and the formation mechanism of PANI nanostructures was discussed. Finally, we will demonstrate the potential of these PANI-DPA nanostructures in corrosion applications.

2. Experimental section

2.1. Preparation of PANI

Benzylphosphonic acid (BPA) and decylphosphonic acid (DPA) were prepared by the Michaelis-Arbuzov reaction.[25] The interfacial reactions were carried out in 20 ml vials. All synthesis were performed with a fixed concentration of aniline in the organic phase (0.37 M) and the concentration of DPA in the aqueous phase was varied to get an aniline / DPA molar ratio between 33 and 3700. All results presented in this paper, otherwise stated, corresponds to an amount of DPA in the aqueous phase around the cmc. Typically, 0.9

[a] Laboratoire MAPIEM EA 4323 ,SeaTech-Ecole d'ingénieurs, Université de Toulon BP 20132, 83957 La Garde Cedex, France

Electronic Supplementary Information (ESI) available: [UV-visible spectra of the solubilization method to determine the critical micellar concentration of decyl and benzylphosphonic acid. Images of PVB coated steel panel without and with PANI at different concentrations (0.5, 2 and 15 wt %) around the scribe area after 20 days salt spray testing. EDS analysis of the defect area of PVB coatings loaded with PANI-DPA (a) and with PANI-BPA (b) after 20 days salt spray testing]. See DOI: 10.1039/x0xx00000x

mmol of APS was dissolved in 1 mL of water and added to 9 mL of $1.4.10^{-3}$ mol/L acid solution. 10 ml of a xylene solution containing aniline (3.7 mmol) was gently added to the aqueous solution. The two-phase system was left undisturbed at room temperature for 24 h. The dispersion of PANI in the aqueous phase was precipitated by adding an excess of acetone, filtered and washed several times with distilled water and acetone until the filtrate is colorless and finally dried under vacuum at 40 °C for 24 h. Dedoped PANI (EB) was obtained by treatment with 0.1M NH_4OH solution. Polyvinyl butyral (PVB) -PANI dispersions in ethanol were applied on low-carbon steel (12.5 × 7.5 × 0.3 cm) to give 20±3 µm thick coatings after drying at RT for 48 h.

2.2. Characterization

A Zeiss Supra 40 VP Field Emission Scanning Electron Microscope (SEM) equipped with an energy dispersive X-ray spectroscopy (EDS) probe (Oxford X-max- 20) and a FEI Tecnai TEM working with a LaB_6 electron source (TEM) were used to image the PANI morphology.

Fourier transform infrared (FTIR) spectra were recorded on a FT-IR spectrometer (Nexus, ThermoNicolet) with KBr pellets. For ultraviolet visible (UV-vis) (Shimadzu UV-2501 PC spectrophotometer), PANI was dissolved in NMP by aid of sonication. Thermogravimetric analysis (TGA) was carried out at 10 K min^{-1} in air (100 mL min^{-1}). The corrosion protection performance was evaluated by visual inspection after salt spray test (ASTM B117) and by electrochemical measurement using a PVC tube fixed on the coated steel panels so as to expose an area of 16.3 cm^2. A solution of 3.5 wt% NaCl was taken in the PVC tube and a saturated calomel electrode (SCE) was placed inside the PVC tube. Electrochemical Impedance Spectroscopy (EIS) measurements were carried out using a 273 A potentiostat (EGG/PAR) coupled to a Solartron 1255 frequency response analyser at open circuit potential applying a 5 mV amplitude perturbation in the 20 mHz- 200 kHz frequency range. A conventional three-electrode cell was used consisted of a platinum foil as auxiliary electrode, a saturated calomel reference electrode (SCE) and the coated metal as the working electrode. The open circuit potential (OCP) of the coated steel was measured with respect to SCE. A Varian Spectr AA-800 atomic absorption spectrometer was used to determine the amount of iron in the NaCl solution after 10 days corrosion test.

3. Results and discussion

The two-phase oxidation of aniline was carried out in a glass vial with the aniline dissolved in the top phase of xylene and the APS and DPA (or BPA) in the bottom aqueous phase.

When the reaction is carried out with BPA, streams of yellow-brown material sink gradually into the aqueous phase and finally fill the entire water layer (Fig. 1A). Nanofibers are produced with a fiber diameter in the range 70-100 nm (Fig. 2A,C), consistent with the literature values of 30-120 nm for average diameter [9]. When the reaction is carried out with DPA in the aqueous phase (Fig. 1B), yellow-brown polyaniline appears at the interface after a short induction time (~ 1 min); After 40 min, the aqueous phase turns into dark green polyaniline dispersion with no obvious precipitate.

As the reaction proceeds, the organic layer becomes reddish orange indicating migration of aniline oligomers. From TEM image (and also SEM image for which the internal cavity in broken nanotubes is visible), it is demonstrated that the PANI products obtained are nanotubes with a small fraction of nanorods and globules (Fig. 2B,D).

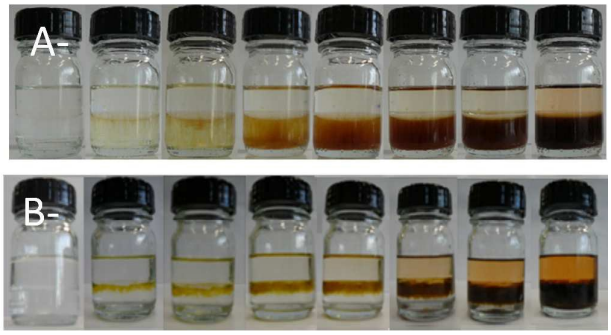

Fig. 1 Snapshots showing interfacial polymerization of aniline in a water/xylene system. From left to right, the reaction times are 0, 2, 5, 10, 15, 30, 40 and 60 min, respectively. The top layer is aniline dissolved in xylene; the bottom layer is an aqueous solution of APS and 1.4 mM DPA (A) or BPA (B).

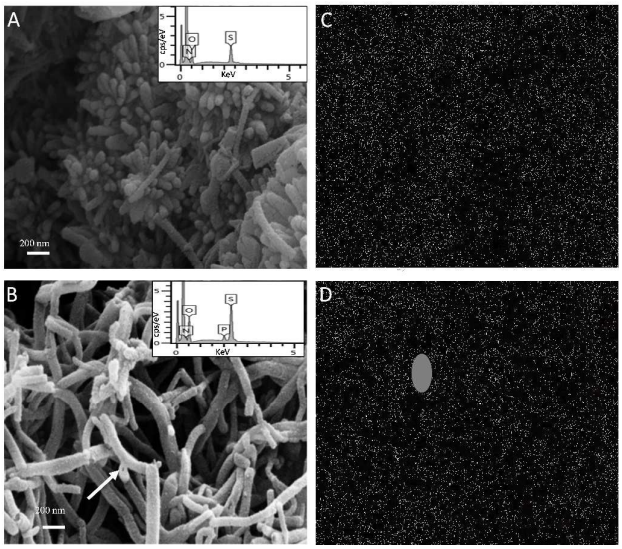

Fig. 2 SEM (EDS pattern in inset) (A,B) and TEM images (C,D) of the product obtained when the reaction is carried out with BPA (A,C) and DPA (B,D) in the aqueous phase. Cavity of nanotube is indicated by the arrow in SEM image Fig.2B.

The outer and inner diameters of the nanotubes are in the ranges 160-240 nm and 50-100 nm, respectively. EDS (inset of Figure 2) indicates that both sulfur and phosphor are present when the reaction is carried out with DPA (P/S atomic ratio ~0.7 and doping level, (P+S)/N, ~32%) while sulfur but no phosphor is present with BPA (doping level, S/N, ~60%). We can thus conclude that DPA is a dopant for polyaniline (together with hydrogensulfate and/or sulfate anions) while BPA is not a dopant of polyaniline.

The yield of polyaniline prepared with DPA in the aqueous phase is around 23 % which is comparable to that by traditional synthesis with the same aniline:APS molar ratio. FTIR spectra of the purified products substantially differ from each other (Fig. 3A). The quinonoid and benzene ring stretching bands at 1568 and 1498 cm^{-1}, respectively, shift to higher wavenumbers (1582 and 1515 cm^{-1}) in the spectrum of PANI-BPA. Bands at 1637, 1447, 1416, 1208 and 1138 cm^{-1} in the spectra of the products obtained with BPA have been previously assigned to ortho-coupled aniline units and phenazine like units.[26] Also, the peaks at 860 and 850 cm^{-1} are characteristic of polysubstituted aniline rings.[27] All these peaks are strongly reduced in the spectra of the products prepared with DPA. With DPA, the aniline constitutional units are linked with a strong preference for the para-position as suggested by the presence of a strong peak at 825 cm^{-1}. On the other hand, the strong peak at 1140 cm^{-1}, associated with $-NH^{\cdot+}=$ structure, confirms that the nanotubes are partially conductive. The peak located at 1040 cm^{-1} indicates the presence of sulfonate groups attached to the aromatic rings.

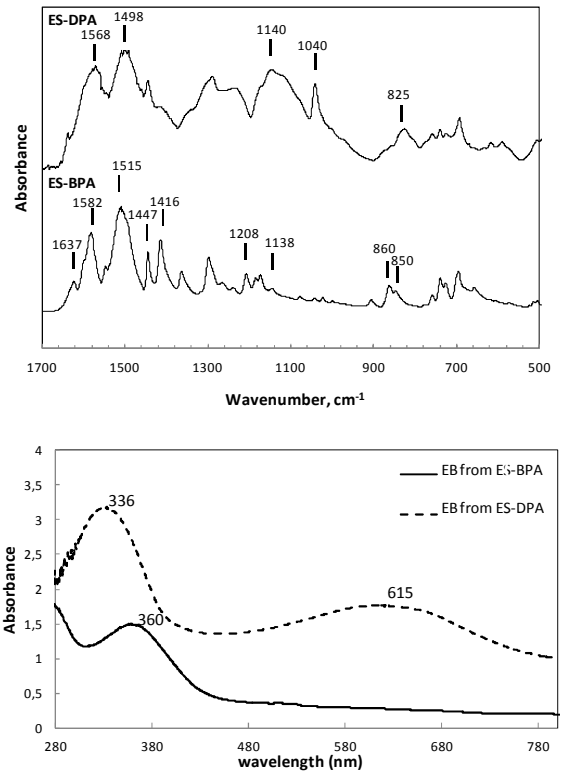

Fig. 3 FTIR (A) and UV-visible (B) spectra of the purified products obtained when the reaction is carried out with DPA (top) or with BPA (bottom) in the aqueous phase. For UV-vis analysis, dedoped PANIs were obtained because the products were dissolved in N-methylpyrrolidone.

This is supported by the presence of sulfur in the PANI bases (S/N = 0.09 and 0.27 for the dedoped PANI-DPA and dedoped PANI-BPA, respectively). It is well known that ring sulfonation is promoted under weakly acid (as it is the case here) or alkaline conditions and not under strongly acidic conditions.[26] The single absorption maximum at 360 nm in the UV-vis spectrum of the product prepared with BPA also supports the formation of aniline oligomers with absence of conjugation (Fig. 3B). In contrast, the UV-vis spectrum of the product obtained with DPA in the aqueous phase shows the characteristic absorptions of PANI base with two maxima located at 336 and 615 nm.[26] From FTIR and UV-vis spectroscopy, the main product with BPA in the aqueous phase is oligoaniline. This result in a much lower yield (5 %) compared to PANI-DPA due to extensive loss of material during the repeated acetone washings. The conductivity of the product prepared with BPA in the aqueous phase is low, $1.0x10^{-6}$ S/cm, because it is mainly composed of non-conducting oligomers. The conductivity increases by more than two decades when the reaction is carried out with DPA ($1.4x10^{-4}$ S/cm) but remains low compared to the typical conductivity of PANI (1-10 S/cm). The reduced conductivity is a consequence of the presence of non-conducting oligomers in the final product and to the ring sulfonation which is majored in the present conditions.[28] The common nanofiber morphology for PANI prepared by IP is observed by using BPA in the water phase while uncommon nanotube morphology was obtained for PANI prepared with DPA. DPA spontaneously forms vesicles in the water phase[29] while BPA does not self-organize in water. It was found that the nanotube morphology was obtained by carrying out IP with a DPA concentration well below the cmc (cmc=1.4mM as determined by solubilization method, see supporting information Figs. S1,S2). This proves that nanotubes are not derived from DPA vesicles. The nanotube morphology was obtained in the whole DPA concentration range investigated. IP carried out without added acid resulted in various nanostructures in agglomerated form: nanorods, nanosheets, nanospheres and nanotubes (Fig. 4). Compared to IP using BPA in the aqueous phase, the kinetics of oligomer-based aggregates migration into the aqueous phase acidified with DPA is significantly reduced, which could play an important role in the formation of PANI nanotubes. Also, the resulting PANI is doped with DPA (and not BPA) which is expected to decrease their hydrophilic character and, consequently, their transfer to the aqueous phase. The acidity profiles for IP with DPA shows the three reaction phases typically observed when oxidation of aniline is carried out in a solution of weak acids[2] (Fig. 5A). The evolution of the morphology of intermediates and products was observed by AFM (Fig. 5B). Nanospheres are first deposited on Si windows followed by a progressive change of the 3D morphology to 1D nanofiber morphology during the induction period. The diameter of nanofiber was around 80 nm at the end of the induction period (30 min). The transition in the morphology from nanofiber to nanotube occurs concomitantly with the rapid drop of pH taking place at pH<2.5. It is accompanied by a rapid increase in the diameter of 1D nanostructure from 80 nm to 200 nm. This suggests that PANI nanotubes are formed by the dissolution of the oligoaniline cores induced by their protonation at pH<2. The nanofibers formed with BPA in the aqueous phase leaves the reactive interface before the critical pH (below 2.5[2]) for the growth of long chains of para linked units is reached. Hence, oligoaniline nanofibers are almost

exclusively produced. Our results support the concept based on crucial template role of in situ formed and precipitated oligoanilines in the formation of PANI nanotubes by falling-pH self-assembly method.

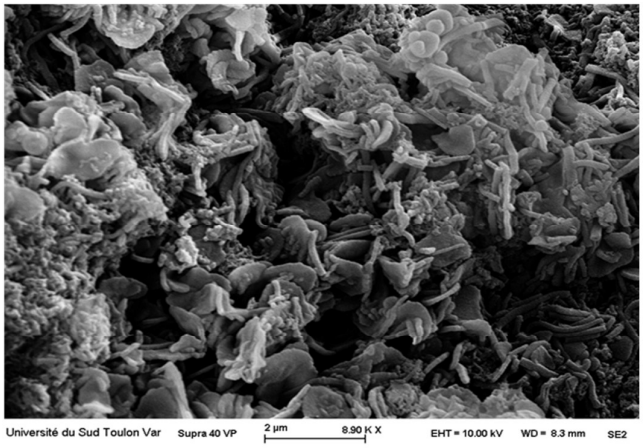

Fig. 4 SEM image of the product obtained when the reaction is carried out without added acid in the aqueous phase.

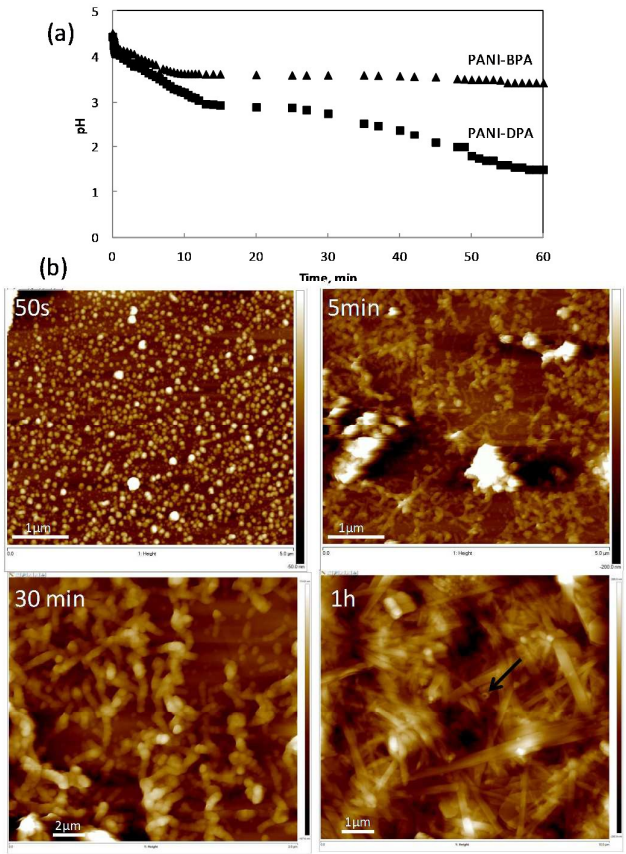

Fig. 5 (A) Acidity profiles during IP with DPA and BPA in the aqueous phase and (B) AFM images of the oxidation products deposited on silicon windows after different reaction times with DPA in the aqueous phase. The internal cavity of a nanotube is marked by an arrow on the AFM image obtained after the reaction time t=1h.

TGA indicated a higher thermal stability of PANI-DPA compared to PANI-BPA with a decomposition temperature (noted as the temperature at 10% weight loss) exceeding by 80°C the value found for PANI-BPA (Fig. S3). ES form is an anion reservoir which can release anions in a smart way when damage is produced on the surface of the coating.[30] It is well established that phosphono groups interact strongly with metal oxides. The inhibitive properties of DPA may thus provide further protection to the base metal. Preliminary corrosion tests were performed on mild steel coated with PVB films loaded with 0 to 15 wt% PANI. The best protective performance was obtained when the amount of PANI was 0.5 wt%. The optimal wt% of PANI incorporated into a polymer binder is typically around 1-10 wt%.[31] The low optimal content of PANI could be related to the large specific surface area of the one-dimensional nanostructured PANI which increases the efficiency of the anodic protection mechanism of steel by PANI. Fig. 6 shows the impedance spectra of the mild steel samples coated with pristine PVB film and PVB films loaded with 0.5 wt% of polyaniline pigment. The spectra were taken after 10 and 20 days exposure in 3.5% NaCl solution. The neat PVB films appeared severely degraded after 10 days exposure times and they were not thus characterized for longer exposure times. The low frequency (LF) impedance modulus represents the global resistance of the system ($|Z|_{0.02\ Hz} \sim Rs + Rp + Rct$ with Rs, the electrolyte resistance, Rp, the pore resistance and Rct the charge-transfer resistance) and thus, the value of impedance at low frequency can be used as an estimation of the overall protection properties for the coatings.[32] The values of low frequency impedance remained in the order of $10^6\ \Omega.cm^2$ for the steel coated with PVB loaded with PANI-DPA and PANI-BPA, and are two orders of magnitude higher than the steel coated with neat PVB films. The electrochemical response of the coating is represented at high frequencies (typically 10^5-10^4 Hz) while relaxation processes occurring closer to the metal surface (response of a passive or inhibitive layer and/or corrosion processes) are revealed in the EIS spectra at lower frequencies. The EIS response of the films containing PANI-DPA appears different from those containing PANI-BPA but the difference is mainly represented in the mid and low frequency range of the EIS plots. This suggests that the barrier properties of the films loaded with the two types of PANI pigments are quite the same but that these two pigments behave differently concerning their active corrosion protection mechanism.

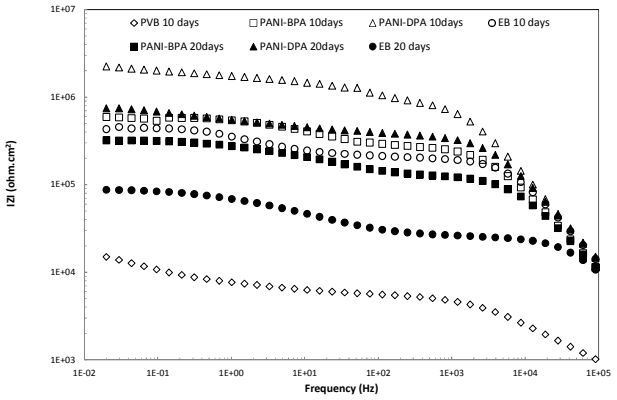

Fig. 6 Impedance spectra of steel specimens coated with PVB coatings only and PVB coatings loaded with 0.5 wt% of PANI-BPA, PANI-DPA or EB after 10 and 20 days of immersion in 3.5 wt% NaCl solution.

During the exposure time, steel coated with PVB films loaded with PANI-DPA has highest LF impedance values compared to those loaded with PANI-BPA. PANI-DPA pigments thus offered the best active corrosion protection for steel. The EIS response for PVB coatings loaded with undoped PANI (EB) is also shown in Fig.6. The results indicate that the corrosion protection by undoped PANI is not as good as that of doped PANIs. This suggests that the corrosion protection mechanism results from the galvanic interaction between doped (conductive) PANI and metal substrate.

The variation of OCP values with immersion time in 3.5 % NaCl solution for studied systems is shown in Fig. 7. The OCP values for PVB coatings loaded with PANI-DPA are found to shift from -0.6V vs SCE to -0.2 V vs SCE gradually up to one day immersion and remained in the same value up one week immersion. Such PANI-BPA coatings showed a much smaller shift in noble direction and attains about -0.5 V vs SCE after one week immersion.

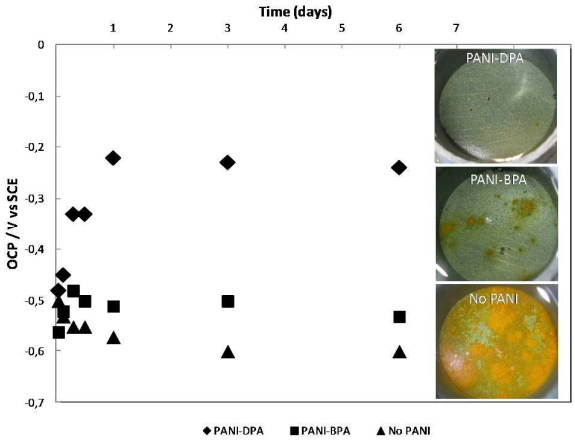

Fig. 7 Variation of OCP with time for PVB coated steel in 3.5 % NaCl solution without PANI, with PANI-BPA and with PANI-DPA. The insets represent the optical photos of the samples taken after a 1-week immersion test in corrosive medium.

On comparing OCP values, the PANI-DPA containing coatings have shown a larger shift in noble direction (ennoblement) which supports a better passivation of steel by polyaniline with DPA. After one week immersion in 3.5 % NaCl solution, the neat PVB coated steel appears severely corroded while the PVB film loaded with PANI-DPA resulted in the best corrosion performance with no corrosion appearing on the surface. Corrosion process was also monitored by measuring the concentration of the iron ions released after exposure to aqueous solutions containing 3.5 wt% of NaCl for 10 days (Fig. 8). The results showed that coatings with DPA doped polyaniline pigments offered the best protection efficiency.

Coatings were artificially scratched and subjected to salt spray testing for 20 days**.** To evaluate scribe creep corrosion, the organic layer was carefully removed with ethanol using a stiff brush. The rust creep was less pronounced in all the systems with 0.5 wt % PANI than in the PVB film without PANI (Fig. 9). The propagation of corrosion from either side of scribe was less pronounced with PANI-DPA pigment than with PANI-BPA pigment. EDS analysis of the scribed region of PANI-DPA based coatings revealed the presence of phosphorus which confirms that DPA dopant is released and contributes to the surface blocking by forming insoluble complex salts with iron such as those reported by treating carbon steel with laurylphosphonic acid and ethyllaurylphosphonate.[33] Hydrogensulfate and/or sulfate anions, that are the dopant ions for PANI-BPA (and not BPA) do not form insoluble complexes with iron ions. This is why S element could not be detected by EDS in the damaged area. Thus, PANI-BPA, contrary to PANI-DPA, does not provide self-healing action for defects. A low amount of PANI (0.5 wt%) offered a more efficient self-healing action than high amounts of PANI (Fig. S4). The low optimal content of PANI can be related to the large PANI/steel interfacial area offered by the nanotubular and nanofibrillar morphology of PANI-DPA and PANI-BPA, respectively. The calculated specific surface areas (SSA) based on geometric considerations were around 26 m²/g and 38 m²/g for PANI-DPA nanotubes (SSA= $\frac{4}{\rho(d_e - d_i)}$) and PANI-BPA nanofibers (SSA= $\frac{4}{\rho.d}$), respectively (d_e, $d_{i\ and\ d}$ the external and internal diameter of nanotubes and diameter of nanofibers determined by TEM and ρ=1.245 g/cm^3, the density of PANI[34]). This suggests that the higher efficiency of PANI-DPA nanotubes is not related to the different morphology (nanotube vs nanofiber) but rather the corrosion inhibitive properties of DPA dopant.

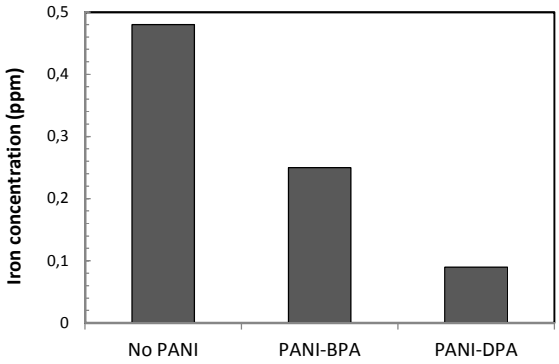

Fig. 8 Iron concentration in the 3.5% NaCl solution after 10 days immersion test of steel specimens coated with PVB coatings only and with PVB coatings loaded with 0.5 wt% of PANI-BPA or PANI-DPA.

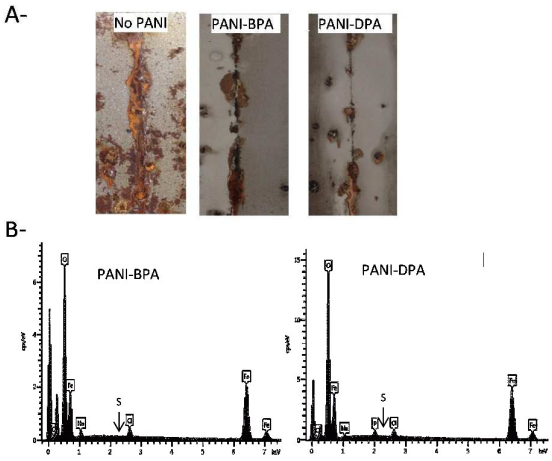

Fig. 9. Steel specimens with artificial damages A- Optical photos taken after removal of PVB around a scribe in the PVB coated steel specimens without and with 0.5 wt % PANI after 20 days of salt spray test. B- EDS analysis of the corrosion products in the damaged area for PVB coated steel loaded with PANI-BPA and PANI-DPA (both at 0.5 wt%) at the end of the salt spray test.

4. Conclusion

The interfacial polymerization is known to produce typically nanofibers. We report here a successful synthesis of polyaniline nanotubes by IP using decylphosphonic acid in the aqueous phase. It is proposed that aniline oligomer nanofibers, rather than aniline-DPA salt micelles, serve as template for the nucleation of PANI nanotubes. DPA played a role in the growth of nanotubes by mitigating the kinetics of oligomer-based aggregates migration into the aqueous phase. Due to the healing properties and the anodic mechanism, PANI doped DPA performed the best for corrosion protection of mild steel.

Acknowledgements

The authors gratefully acknowledge the Ministère de l'Education et de la Recherche for his financial support. The authors also thank Dr. Ahmad Fahs for his valuable assistance for AFM measurements.

References

1 S. Iijima, *Nature* 1991, **354**, 56.
2 J. Stejskal, I. Sapurina, M. Trchová, *Progress Polym. Sci.* 2010, **35**, 1420-1481.
3 C. Laslau, Z. Zujovic, J. Travas-Sejdic, *Prog. Polym. Sci.* 2010, **35**, 1403-1419.
4 H.D. Tran, J.M. D'Arcy, Y. Wang, P.J. Beltramo, V.A. Strong, R.B. Kaner, *J. Mater. Chem.* 2011, **21**, 3534-3550.
5 G.C. Marjanovic, *Synth. Met.* 2013, **177**, 1-47.
6 J.C. Michaelson and A.J. McEvoy, *Chem. Commun.* 1994, **79**
7 C.G. Wu and T. Bein, *Science* 1994, **264**, 1757-1759.
8 X. Zhang, W.J. Goux and S.K. Manohar, *J. Am. Chem. Soc.* 2004, **126**, 4502-4503.
9 J. Huang and R.B. Kaner, *J. Am. Chem. Soc.* 2003, **126**, 851-855.
10 J. Liu, Y. Lin, L. Liang, J.A.Voigt, D.L. Huber, Z.R. Tian, E. Coker, B. Mckenzie and M.J. Mcdermott, *Chem. Eur. J.* 2003, **9**, 605-611.
11 A.G. MacDiarmid, W.E. Jones, I.D. Norris, J. Gao, A.T. Johnson, N.J. Pinto, J. Hone, B. Han, F.K. Ko, H. Okuzaki and M. Laguno, *Synth. Met.* 2001, **119**, 27-30.
12 H.X. He, C.Z. Li and N.J. Tao, *Appl. Phys. Lett.* 2001, **78**, 811-813.
13 J. Huang and R.B. Kaner, *Chem. Commun.* 2006, 367-376.
14 J. Chen, J. Yang, X. Yan and Q. Xue, *Synth. Met.* 2010, **160**, 2452-2458.
15 R. Li, Z. Chen, J. Li, C. Zhang and Q. Guo, *Synth. Met.* 2013, **171**, 39-44.
16 X. Sun, S. Dong and E. Wang, *Chem. Commun.* 2004, 1182
17 J. Huang, S. Virji, B.H. Weiller and R.B. Kaner, *J. Am. Chem. Soc.* 2002, **125**, 314-315.
18 X. Zhang, R. Chan-Yu-King, A. Jose and S.K. Manohar, *Synth. Met.* 2004, **145**, 23-29.
19 X. Zhang and S. Manohar, *Chem. Commun* 2004, 2360.
20 N. Wang, H. Li, T.Y. Chen, J.T. Wang and Q. Shen, *Mater. Lett.* 2014, **137**, 203-205.
21 S. Liu, K. Zhu, Y. Zhang and J. Xu, *Polymer* 2006, **47**, 7680-7683.
22 J. Wang, J. Wang, X. Zhang and Z. Wang, *Macromol. Rapid Commun.* 2007, **28**, 84.
23 Y. He and J. Lu, *React. Funct. Polym.* 2007, **67**, 476-480.
24 Q. Sun and Y. Deng, *Mater. Lett.* 2008, **62**, 1831-1834.
25 B. A. Arbusov *Pure Appl. Chem.* 1964, **9**, 307-335.
26 J. Stejskal, I. Sapurina, M. Trchová and E.N. Konyushenko, *Macromolecules* 2008, **41**, 3530-3536.
27 L. Zhang, Z.D. Zujovic, H. Peng, G.A. Bowmaker, P.A. Kilmartin and J. Travas-Sejdic, *Macromolecules* 2008, **41**, 8877-8884.
28 J. Stejskal and M. Trchová, *Polym. Inter.* 2012, **61**, 240-251.
29 P. Walde, M. Wessicken, U. Rädler, N. Berclaz, K. Conde-Frieboes and P.L. Luisi, *J. Phys. Chem. B* 1997, **101**, 7390-7397.
30 J.E. Pereira da Silva, S.I. Cordoba de Torresi and R. M. Torresi *Corros. Sci.* 2005, **47**, 811-822.

31 G. Gupta, N. Birbilis, A.B. Cook and A.S. Khanna *Prog. Org. Coat.* 2013, **57**, 256-267.
32 J.M. McIntyre and H.Q. Pham, *Prog. Org. Coat.* 1996, **27**, 201–207.
33 X.H. To, N. Pebere, N. Pelaprat, B. Boutevin and Y. hervaud, *Corros. Sci.* 1997, **39**, 1925-1934.
34 J. Stejskal, R.G. Gilbert, *Pure Appl. Chem*. 2002, **74**, 857–867.